SOĞUK METAL TRANSFER (CMT) KAYNAĞI İLE BİRLEŞTİRİLEN AA6061-T6 ALÜMİNYUM ALAŞIMININ MİKROYAPI VE MEKANİK ÖZELLİKLERİNİN ÇOK YÖNLÜ OPTİMİZASYONU

Dr. Öğr. Üyesi, Murat ŞEN (Birinci yazar)1/ Dr. Öğr. Üyesi, Erman FERİK (İkinci yazar)2
1Marmara Üniversitesi, Teknoloji Fakültesi, Makine Mühendisliği Bölümü, Tasarım ve İmalat Anabilim Dalı, murat.sen@marmara.edu.tr, 0000-0003-2216-245X
2Marmara Üniversitesi, Teknoloji Fakültesi, Metalurji ve Malzeme Mühendisliği Bölümü, Mekanik Metalurjisi Anabilim Dalı, erman.ferik@marmara.edu.tr, 0000-0002-9694-5732

Özet

Günümüzde otomotiv, havacılık ve uzay endüstrisinde düşük maliyetli, dayanımı yüksek, daha hafif ve yüksek verimli kaynak yöntemlerine olan gereksinim artmıştır. Bu özellikleri sağlayan CMT kaynağı alüminyum alaşımlarının kaynağında öne çıkmaktadır. Bu nedenle, yapılan çalışmada AlMg4,5Mn dolgu teli kullanılarak AA6061-T6 sacların birleştirilmesinde soğuk metal transferi (CMT) kullanılmıştır. Farklı torç açısı, koruyucu gaz debileri ve kaynak hızı kullanılarak yapılan kaynaklı birleştirmelerin mekanik özellikleri ve mikroyapıları incelenmiştir. Optimum proses parametreleri Taguchi deneysel tasarım metodu kullanılarak elde edilmiştir. Çekme dayanımı için optimum seviyeler A2-B2-C1 (70° - 12 L/dak - 40 cm/dak), sertlik için ise A2-B1-C1 (70° - 8 L/dak - 40 cm/dak) olarak belirlenmiştir. Ayrıca ANOVA yardımıyla proses parametrelerinin sonuçlara katkısı hesaplanmıştır. Yapılan deneysel çalışmanın sonucunda, mekanik özellikler üzerinde en etkili parametreler sırasıyla kaynak hızı, torç açısı ve koruyucu gaz debisi şeklinde olduğu görülmüştür. Kaynak hızı arttıkça mekanik özelliklerin azaldığı gözlenmiştir. Yüksek gaz debisi ve torç açısının mekanik özellikleri olumsuz yönde etkilediği tespit edilmiştir.

Anahtar Kelimeler: CMT Kaynağı, AA6061-T6, Mekanik Özellikler, Mikroyapı, Taguchi Optimizasyonu

THE MULTI-DIMENSIONAL OPTIMIZATION OF MICROSTRUCTURE AND MECHANICAL PROPERTIES OF AA6061-T6 ALUMINUM ALLOY JOINED BY COLD METAL TRANSFER (CMT) WELDING

1Marmara University, Faculty of Technology, Department of Mechanical Engineering, Design and Manufacturing, murat.sen@marmara.edu.tr, 0000-0003-2216-245X
2Marmara University, Faculty of Technology, Department of Metallurgical and Materials Engineering, Mechanical Metallurgy, erman.ferik@marmara.edu.tr, 0000-0002-9694-5732

Abstract

Nowadays the automotive, aviation, and space industries increasingly seek low-cost, high-strength, lighter, and more efficient welding processes. CMT welding, which gives these qualities, shines out when joining aluminum alloys. In the investigation, cold metal transfer (CMT) was used to join AA6061-T6 sheets with AlMg4.5Mn filler wire. The mechanical characteristics and microstructures of welded joins generated at various torch angles, shielding gas flow rates, and welding speeds were examined. The Taguchi experimental design approach was used to determine the most optimal process parameters. The optimum levels for tensile strength were determined as A2-B2-C1 (70° - 12 L/min - 40 cm/min) and for hardness as A2-B1-C1 (70° - 8 L/min - 40 cm/min). In addition, the contribution of the process parameters to the findings was evaluated using ANOVA. The experimental study revealed that the most effective parameters on mechanical properties were welding speed, torch angle, and shielding gas flow rate. The mechanical characteristics decreased as the welding speed increased. High gas flow rate and torch angle were shown to have a negative impact on mechanical characteristics.

Keywords: CMT Welding, AA6061-T6, Mechanical Properties, Microstructure, Taguchi Optimization

INTRODUCTION

In recent years, lighter vehicle manufacture has emerged as one of the most successful methods for lowering fuel consumption and emissions [1, 2]. Some metal alloy classes, such as aluminum alloys, have mechanical qualities similar to steel types and are used in a variety of applications due to their light weight. Aluminum alloys are also used in a variety of applications due to their corrosion resistance and aesthetic appear increasingly used in transportation industries, including aviation and automotive [3-9].

Aluminum alloys contain alloying elements such as Mg, Si, Zn, Mn, Cu, and so on, allowing aluminum metal to be used for a variety of demanding applications. The 6xxx aluminum series contains magnesium and silicon as the main alloying elements. Because of its strength, lightness, ductility, formability, and corrosion resistance, 6061-T6 aluminum alloy is widely employed in a variety of industries, including aviation and maritime transportation [10-25].

Aluminum alloys' strong thermal conductivity, thermal expansion coefficients, rapid solidification rates, and wide solidification temperature range all contribute to welding issues such as porosity, hot fractures, lack of fusion, and distortion. Aluminum alloys, particularly 6061, which gain strength by precipitation hardening, have been shown to undergo phase transitions and lose strength as a result of the heat input created by the welding process. Innovative welding processes, including cold metal transfer (CMT) and friction stir welding, have been developed to join aluminum alloys in recent years [26-31].

Fronius invented the cold metal transfer (CMT) process in 2005 as an improvement to metal inert gas (MIG) welding. It is frequently used to join aluminum alloys, galvanized thin steel sheets, and dissimilar metals and alloys because of its benefits over other welding processes, such as reduced spatter rate and porosity, enhanced arc stability, regulated molten metal transfer, and good gap-bridging capacity [32-41].

There are other comparable research on this topic in the literature. Koli et al. investigated the optimization of process parameters by welding AA6082-T6 and AA6061-T6 sheets using the CMT welding method with three different welding current, welding speed, and shielding gas flow rate combinations. And the welding speed was discovered to be the most effective. In the investigation done by Raj et al., AA6082-T6 sheets were welded using the CMT welding method with three different welding current, welding speed, and arc length correction factor combinations, and the process parameters were adjusted [42-43].

The weldability of 6061-T6 aluminum alloy sheets used in aviation, aerospace, and other industries was investigated using the CMT method in this study, as well as the effect of welding parameters on mechanical properties and microstructure using Taguchi, ANOVA, response surface, and regression analysis techniques. The tensile test results for joints were evaluated, and microhardness values were measured. To analyze the weldability of 6061-T6 series aluminum sheets using the CMT method, the micro and macro structures of the samples, as well as SEM photos, were investigated, and EDS analysis was done.

1. METHOD

1.1. Materials

In the investigation of cold metal transfer (CMT) welding, 6061-T6 aluminum alloy, which is frequently preferred in critical sectors such as defense, automotive, aviation and construction due to its high mechanical properties and corrosion resistance, was used. 6061-T6 samples were produced by rolling method and are 1.5 mm plates. Prior to the welding process, the aluminum plates were cut to dimensions of 200 × 200 mm and subsequently cleaned with acetone to eliminate surface contaminants such as dirt and oil. Spectrometric analysis and mechanical properties of 6061-T6 aluminum alloy is given in Table 1 and 2. In all welding processes, AlMg4.5Mn filler rods were employed, selected for their compatibility with the chemical composition of the base metal (Table 3 and 4).

Table 1. Chemical composition of 6061-T6 aluminum alloy (wt%).

Elements	Si	Fe	Mn	Mg	Cu	Cr	Ni	Zn	Ti	Al
Content	0.64	0.367	0.114	0.8	0.275	0.193	0.005	0.157	0.029	97.4

Table 2. Mechanical properties of 6061-T6 aluminum alloy.

Tensile strength (MPa)	Yield strength (MPa)	Elongation (%)	Hardness (HV)
334	295	13	110

Table 3. Chemical composition of AlMg4.5Mn filler rods (wt%).

Elements	Mg	Mn	Cr	Si	Fe	Al
Content	5	0.8	0.2	<0.4	<0.4	Kalan

Table 4. Mechanical properties of AlMg4.5Mn filler rods.

Tensile strength (MPa)	Yield strength (MPa)	Elongation (%)
>250	>120	>16

1.2. Methods

A schematic representation of the welding process is given in Fig. 1. The CMT process was carried out automatically using the butt-joint configuration on the Fronius A-4600 CMT welding machine. Pure argon (100% Ar) was used as the shielding gas during the welding process to prevent oxidation and ensure weld quality. In order to reduce the distortions and cracks that may occur in the samples, a mold system fixed with screws was made and the samples were connected to this mold and the welding process was performed.



Figure 1. A schematic representation of the welding process.

The experimental results for Al 6061 aluminum alloy was analyzed in terms of microstructure and mechanical properties. Design of Experiments (DOE), a statistical approach frequently used in process optimization, was used in the study [44-48]. The parameters used in the study are shown in Table 5. In determining the control factors and levels, the most frequently used welding process parameters and values in the literature were selected. Accordingly, three control factors and levels were determined in welding process. Experimental studies were carried out in accordance with the Taguchi L9 orthogonal design matrix (Table 6). All tests were

validated by repeating three times on a total of 27 parts. Minitab 22 software was used to evaluate the test results.The effects of factors and levels on the results were examined with signal to noise ratio (SNR). In order to have high mechanical properties after welding, tensile strength and hardness values must be high. Therefore, "The higher - the better" was used in calculating the signal to noise (S/N) ratio in the experimental design.The effect of each factor on the results was determined using analysis of variance (ANOVA). The percentage contribution and variance ratio for each control factor were computed. The ANOVA was conducted at a 95% confidence level to ensure statistical reliability.

Table 5. Input factors and levels.

Input factors	Symbol	Levels			Unit
		Level 1	Leve 2	Level 3	
Angle of bevel	A	50	70	90	°
Gas flow rate	B	8	12	16	l/dk
Welding speed	C	40	60	80	cm/dk

Table 6. L9 orthogonal matrix of input and output factors.

Exp. no	Input factors/ Symbol			Output factors	
	A	B	C	Tensile strength (MPa)	Hardness (HV)
1	1	2	1	166.7	82.8
2	1	2	2	163.6	79.9
3	1	3	3	152.5	74.2
4	2	1	2	172.6	85.7
5	2	2	3	169.4	81.4
6	2	3	1	175.1	85.1
7	3	1	3	159.3	80.3
8	3	2	1	177.0	86.4
9	3	3	2	161.6	79.8

In order to determine the mechanical properties of the samples joined with CMT welding, tensile tests were carried out with a 5-ton capacity Shimadzu brand tensile device. Tensile test samples were prepared according to EN 895 standard. The sample dimensions used in the tensile test are given in Fig.2. The experiments were carried out with a test speed of 10 mm/min. The vickers hardness values of each sample were measured with a microhardness tester at 0.5 mm intervals. Measurements were performed under room conditions using a 100-gram load and a pyramid indenter for 10 seconds. Fig. 3 illustrates the specific points on the sample where hardness measurements were performed.

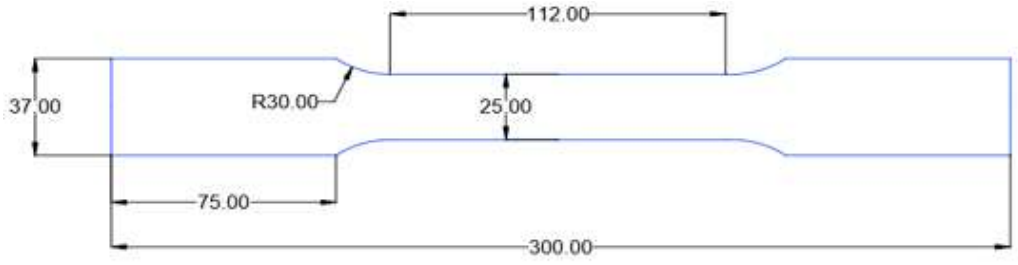

Figure 2. Dimensions of tensile sample (mm)

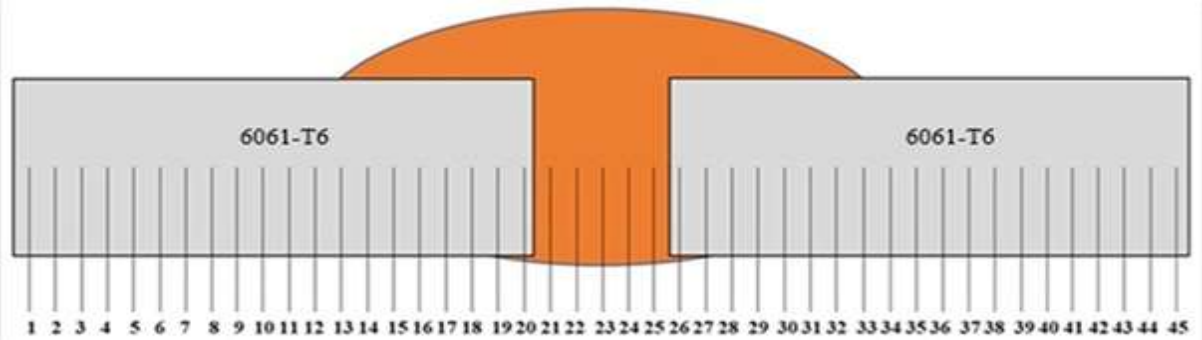

Figure 3. Microhardness measurements of welded samples.

2. RESULTS

The S/N ratios of tensile strength and hardness are given in Table 7. Table 7 shows that the most effective parameters on tensile strength and hardness are welding speed (C), angle of bevel (A) and gas flow rate (B), respectively. Similar studies in the literature confirm the results.

In their study, Raj et al. joined 6061T6 sheet metal by CMT welding using different welding current intensities (80 A, 90 A, and 100 A), welding speeds (6, 9, and 12 mm sec-1) and arc length correction factors (0, 5, -10). The obtained results were analyzed and it was seen that the results obtained by the Taguchi L9 optimization technique were confirmed. The highest strength was obtained with 100 A current, 9 mm/s welding speed, and 10% arc length correction factors. [43]

In welded joints, it is observed that tensile strength and hardness values decrease as the welding speed decreases. Excessive heat input reduces the strength and hardness of the weld zone. Furthermore, mechanical properties obtained after welding with a low torch angle will also be lower. Similarly, a high torch angle negatively affects mechanical properties. Furthermore, the gas flow rate must be optimized. Excessive gas flow reduces tensile strength and hardness. Welding speed is the factor that most significantly affects the mechanical properties of welded joints. Torch angle follows. Gas flow rate has a lesser effect.

In order to reach the highest tensile strength and hardness values in the CMT process, the optimum levels of control factors for tensile strength were determined as A2-B2-C1 (70°-12 L/min-40 cm/min) and for hardness as A2-B1-C1 (70°-8 L/min-40 cm/min). Levels A2-B2-C1 and A2-B1-C1 are not included in the L9 experiment set in Table 6. For this reason, verification tests were carried out using optimum process parameters. As a result of the verification tests, the tensile strength was measured as 182.6 MPa and the hardness was measured as 89.1 HV. These values are higher than the tensile strength and hardness values given in Table 7.

Table 7. S/N ratios of the welded Al 6061 samples.

Output factors	**Tensile strength**			**Hardness**		
Input factors / Symbol	**A**	**B**	**C**	**A**	**B**	**C**
Level 1	44.13	44.41	44.75	37.94	38.37	38.56
Level 2	44.73	44.60	44.40	38.49	38.33	38.25
Level 3	44.39	44.23	44.10	38.29	38.02	37.90
Delta	0.60	0.37	0.66	0.55	0.36	0.66
Rank	2	3	1	2	3	1

The effects of control parameters and process levels on tensile strength and hardness are shown in one-dimensional (1D) graphs (Figure 4 and 5). The 1-D graphs were drawn using minitab 22 software. It can be seen that the graphs of average S/N ratios support the results obtained in Table 5. The peaks of the curves in the graphs show the optimum level for the relevant factor.

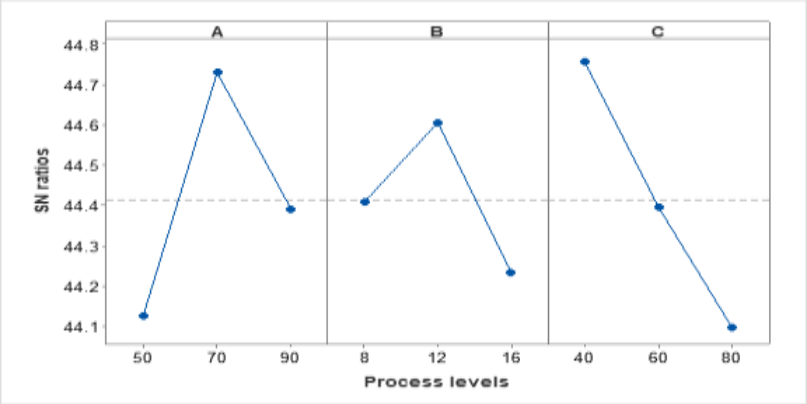

Figure 4. Average S/N ratios for tensile strength.

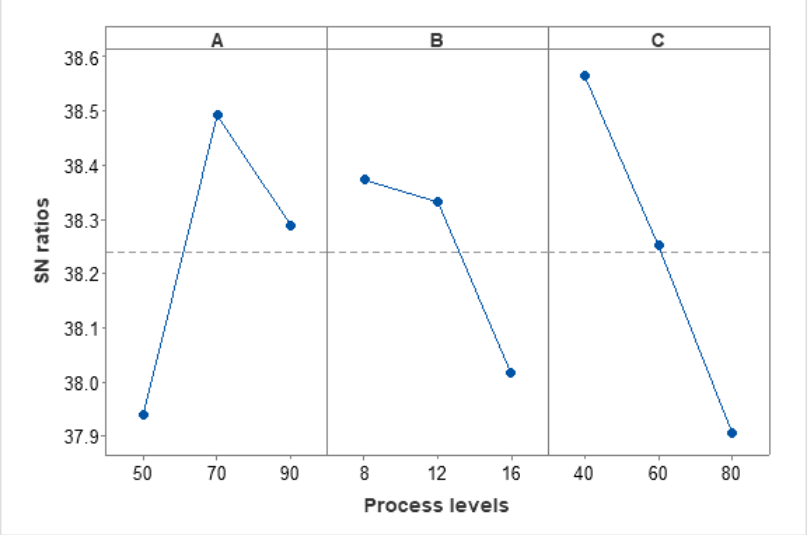

Figure 5. Average S/N ratios for hardness.

The ANOVA results for tensile strength and hardness are given in Table 8 and 9. When ANOVA and Taguchi results are analyzed together, it can be seen that the results are compatible. According to both methods, it was determined that the parameter that most affected the tensile strength and hardness was the welding speed. The contribution of welding speed to tensile strength is around 46% and its effect on hardness is approximately 48%. According to the ANOVA results for tensile strength and hardness, the second most effective parameter was angle of bevel, while the least effective parameter was gas flow rate.

Table 8. Analysis of variance for tensile strength.

Source	Degree of freedom	Sum of squares	Squares average	F ratio	P value	Percentage of contribution (%)
A	2	197.016	98.508	48.90	0.020	38.62
B	2	72.329	36.164	17.95	0.053	14.18
C	2	236.702	118.351	58.75	0.017	46.41
Error (e)	2	4.029	2.014	-	-	0.79
Total	8	510.076	-	-	-	100

Table 9. Analysis of variance for hardness.

Source	Degree of freedom	Sum of squares	Squares average	F ratio	P value	Percentage of contribution (%)
A	2	39.8600	19.9300	44.95	0.022	34.36
B	2	18.807	9.4033	21.21	0.045	16.22
C	2	56.4467	28.2233	63.66	0.015	48.66
Error (e)	2	0.887	0.4433	-	-	0.76
Total	8	116.000	-	-	-	100

2.1. Microstsructure and SEM Images

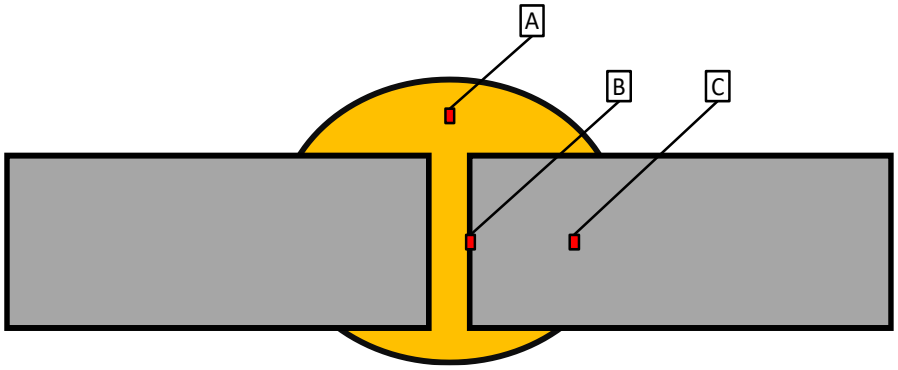

Figure 6. Microstructured regions of welded sample.



A B C

Figure 7. Microstructure images of the sample, a) 6061-T6 Weld Zone (200x) b) 6061-T6 HAZ-Weld Intermediate Transition Zone (200x), c) 6061-T6 HAZ Zone (400x).

The microstructure photos show that the grains are bigger in the nearby portions of the welding process and decrease in size as one approaches closer to the base material. It is hypothesized that Mg and Si elements (usually Mg_2Si) precipitate at the aluminum grain boundaries in the 6061-T6 alloy.

The SEM image taken from the intermediate region of the sample is shown in Figure 8.

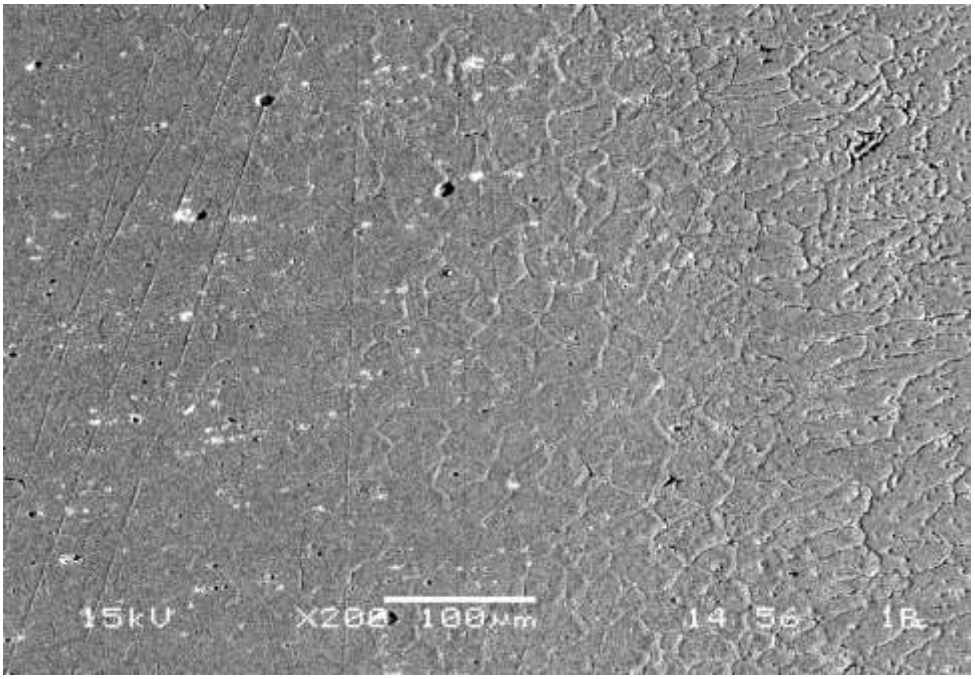

Figure 8. SEM image of welded sample.

The graphic shows that dendritic forms arise as a result of the parent material elements' atomic migration toward the weld zone.

Figure 9 depicts the EDS analysis performed on the sample's intermediate section.

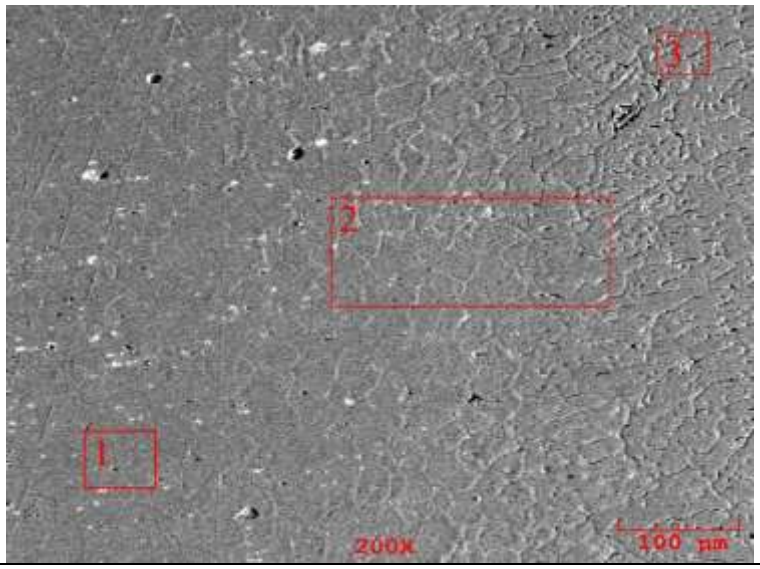

Point taken	Elements (% by weight)				
	Mg	Si	Mn	Cu	Al
1	0,970	0,184	0,362	0,214	98,270
2	0,820	0,261	0,724	0,383	97,812
3	2,363	0,062	0,235	0,996	96,343

Figure 9. EDS analysis of welded sample.

When the EDS data are reviewed, it is clear that the elements diffuse from the weld zone to the 6061-T6 zone when heat is applied, and vice versa.

3. DISCUSSION AND SUGGESTIONS

Çalışma neticesinden elde edilen sonuçlar aşağıda sıralanmıştır:

- It shows that the most effective parameters on tensile strength and hardness are welding speed (C), torch angle (A) and gas flow rate (B), respectively.
- The optimal control parameters for tensile strength were A2-B2-C1 (70°-12 L/min-40 cm/min) and hardness were A2-B1-C1 (70°-8 L/min-40 cm/min). Levels A2-B2-C1, and A2-B1-C1. Tensile strength was measured at 182.6 MPa, while hardness was measured at 89.1 HV.
- In the ANOVA findings for tensile strength and hardness, the second most effective parameter was angle of bevel, whereas the least effective parameter was gas flow rate. Welding speed contributes around 46% to tensile strength and 48% to hardness.
- SEM image and EDS analyses revealed that the heat generated in the weld and HAZ regions changed the microstructure and caused elemental diffusions.

REFERENCES

[1] Rajeshkumar, R., Niranjani, V. L., Devakumaran, K., & Banerjee, K. (2021). Structure-property correlation of weld metal zone and interface regions of cold metal transfer welded dissimilar Al-Mg-Mn alloys joint. *Materials Today: Proceedings*, *46*, 2498-2509.

[2] Yang, S., Zhang, J., Lian, J., & Lei, Y. (2013). Welding of aluminum alloy to zinc coated steel by cold metal transfer. *Materials & Design*, *49*, 602-612.

[3] Rathinasuriyan, C., Muniamuthu, S., Mystica, A., & Kumar, V. S. (2021). Investigation of heat generation during submerged friction stir welding on 6061-T6 aluminum alloy. *Materials Today: Proceedings*, *46*, 8320-8324.

[4] Leon, J. S., Bharathiraja, G., & Jayakumar, V. (2020, October). A review on friction stir welding in aluminium alloys. In *IOP conference series: materials science and engineering* (Vol. 954, No. 1, p. 012007). IOP Publishing.

[5] Zhang, Z., Yang, X., Zhang, J., Zhou, G., Xu, X., & Zou, B. (2011). Effect of welding parameters on microstructure and mechanical properties of friction stir spot welded 5052 aluminum alloy. *Materials & Design*, *32*(8-9), 4461-4470.

[6] Tran, V. X., Pan, J., & Pan, T. (2008). Fatigue behavior of aluminum 5754-O and 6111-T4 spot friction welds in lap-shear specimens. *International Journal of Fatigue*, *30*(12), 2175-2190.

[7] Chowdhury, S. H., Chen, D. L., Bhole, S. D., Cao, X., & Wanjara, P. (2012). Lap shear strength and fatigue life of friction stir spot welded AZ31 magnesium and 5754 aluminum alloys. *Materials Science and Engineering: A*, *556*, 500-509.

[8] Badarinarayan, H., Shi, Y., Li, X., & Okamoto, K. (2009). Effect of tool geometry on hook formation and static strength of friction stir spot welded aluminum 5754-O sheets. *International Journal of Machine Tools and Manufacture*, *49*(11), 814-823.

[9] Rhodes, C. G., Mahoney, M. W., Bingel, W. H., Spurling, R. A., & Bampton, C. C. (1997). Effects of friction stir welding on microstructure of 7075 aluminum. *Scripta materialia*, *36*(1), 69-75.

[10] Singh, V., Murtaza, Q., & Niranjan, M. S. (2024). Microstructure and mechanical properties of CMT welded AA6063-T6/B4C/ES metal matrix composite using ER5356 filler wire. *Materials Today: Proceedings*.

[11] Miller, W. S., Zhuang, L., Bottema, J., Wittebrood, A., De Smet, P., Haszler, A., & Vieregge, A. J. M. S. (2000). Recent development in aluminium alloys for the automotive industry. *Materials Science and Engineering: A*, *280*(1), 37-49.

[12] Šekularac, G., & Milošev, I. (2018). Corrosion of aluminium alloy AlSi7Mg0. 3 in artificial sea water with added sodium sulphide. *Corrosion Science*, *144*, 54-73.

[13] Jiang, Y., & Liu, F. (2019). Effects of Sc or/and Ge addition on microstructure and mechanical properties of as-cast 6016 Al alloy. *Journal of Alloys and Compounds*, *809*, 151829.

[14] Sauvage, X., Bobruk, E. V., Murashkin, M. Y., Nasedkina, Y., Enikeev, N. A., & Valiev, R. Z. (2015). Optimization of electrical conductivity and strength combination by structure design at the nanoscale in Al–Mg–Si alloys. *Acta Materialia*, *98*, 355-366.

[15] Nie, F., Dong, H., Chen, S., Li, P., Wang, L., Zhao, Z., ... & Zhang, H. (2018). Microstructure and mechanical properties of pulse MIG welded 6061/A356 aluminum alloy dissimilar butt joints. *Journal of materials science & technology*, *34*(3), 551-560.

[16] Fridlyander, I. N., Sister, V. G., Grushko, O. E., Berstenev, V. V., Sheveleva, L. M., & Ivanova, L. A. (2002). Aluminum alloys: promising materials in the automotive industry. *Metal science and heat treatment*, *44*(9), 365-370.

[17] Nturanabo, F., Masu, L. M., & Govender, G. (2015, September). Automotive light-weighting using aluminium metal matrix composites. In *Materials Science Forum* (Vol. 828, pp. 485-491). Trans Tech Publications Ltd.
[18] Wang, J., Chen, X., Yang, L., & Zhang, G. (2022). Effect of preheat & post-weld heat treatment on the microstructure and mechanical properties of 6061-T6 aluminum alloy welded sheets. *Materials Science and Engineering: A*, *841*, 143081.
[19] Yadav, R., Sharma, A., Vohra, S., Dewangan, S., & Chowrasia, M. K. (2021). Investigation into defects occurred in friction stir welded joint of 6061-T6 aluminium alloy. *Materials Today: Proceedings*, *46*, 8910-8916.
[20] Gang, W., & Caiqi, Z. (2021, October). Experimental and theoretical study on the bearing capacity of FGC joints for single-layer aluminium alloy lattice shell structures. In *Structures* (Vol. 33, pp. 2445-2458). Elsevier.
[21] Zhu, P., Zhang, Q., Luo, X., Ouyang, Y., & Yin, J. (2020). Experimental and numerical studies on ductile-fracture-controlled ultimate resistance of bars in aluminum alloy gusset joints under monotonic tensile loading. *Engineering Structures*, *204*, 109834.
[22] Xiong, Z., Guo, X., Luo, Y., Zhu, S., & Liu, Y. (2017). Experimental and numerical studies on single-layer reticulated shells with aluminium alloy gusset joints. *Thin-Walled Structures*, *118*, 124-136.
[23] Wang, H., Li, P., & Wang, J. (2021). Shape optimization and buckling analysis of novel two-way aluminum alloy latticed shells. *Journal of Building Engineering*, *36*, 102100.
[24] Wu, Y., Liu, H., Chen, Z., & Liu, Y. (2020). Study on low-cycle fatigue performance of aluminum alloy temcor joints. *KSCE Journal of Civil Engineering*, *24*(1), 195-207.
[25] Liu, H., Ding, Y., & Chen, Z. (2017). Static stability behavior of aluminum alloy single-layer spherical latticed shell structure with Temcor joints. *Thin-Walled Structures*, *120*, 355-365.
[26] Huan, P. C., Wang, X. N., Zhang, J., Hu, Z. R., Chen, W. G., Nagaumi, H., & Di, H. S. (2020). Effect of wire composition on microstructure and properties of 6063 aluminium alloy hybrid synchronous pulse CMT welded joints. *Materials Science and Engineering: A*, *790*, 139713.
[27] Liang, Y., Shen, J., Hu, S., Wang, H., & Pang, J. (2018). Effect of TIG current on microstructural and mechanical properties of 6061-T6 aluminium alloy joints by TIG–CMT hybrid welding. *Journal of Materials Processing Technology*, *255*, 161-174.
[28] Pakdil, M., Çam, G., Koçak, M., & Erim, S. (2011). Microstructural and mechanical characterization of laser beam welded AA6056 Al-alloy. *Materials Science and Engineering: A*, *528*(24), 7350-7356.
[29] Kashaev, N., Ventzke, V., & Çam, G. (2018). Prospects of laser beam welding and friction stir welding processes for aluminum airframe structural applications. *Journal of Manufacturing Processes*, *36*, 571-600.
[30] Tian, Y., Shen, J., Hu, S., Wang, Z., & Gou, J. (2018). Effects of ultrasonic vibration in the CMT process on welded joints of Al alloy. *Journal of Materials Processing Technology*, *259*, 282-291.
[31] Yang, S., Wang, Y., Yang, X., Lu, X., Li, M. V., & Zhu, X. (2024). Effect of softening of 6082-T6 aluminum alloy CMT welded joints on mechanical properties and fracture behavior. *Journal of Manufacturing Processes*, *124*, 1567-1582.
[32] Furukawa, K. (2006). New CMT arc welding process–welding of steel to aluminium dissimilar metals and welding of super-thin aluminium sheets. *Welding international*, *20*(6), 440-445.
[33] Cao, R., Yu, G., Chen, J. H., & Wang, P. C. (2013). Cold metal transfer joining aluminum alloys-to-galvanized mild steel. *Journal of materials processing technology*, *213*(10), 1753-1763.
[34] Zhang, H. T., Feng, J. C., He, P., Zhang, B. B., Chen, J. M., & Wang, L. (2009). The arc characteristics and metal transfer behaviour of cold metal transfer and its use in joining aluminium to zinc-coated steel. *Materials Science and Engineering: A*, *499*(1-2), 111-113.

[35] Meco, S., Pardal, G., Eder, A., & Quintino, L. (2013). Software development for prediction of the weld bead in CMT and pulsed-MAG processes. *The International Journal of Advanced Manufacturing Technology*, *64*(1), 171-178.
[36] Kumar, N. P., Vendan, S. A., & Shanmugam, N. S. (2016). Investigations on the parametric effects of cold metal transfer process on the microstructural aspects in AA6061. *Journal of Alloys and Compounds*, *658*, 255-264.
[37] Chen, M., Zhang, D., & Wu, C. (2017). Current waveform effects on CMT welding of mild steel. *Journal of Materials Processing Technology*, *243*, 395-404.
[38] Feng, J., Zhang, H., & He, P. (2009). The CMT short-circuiting metal transfer process and its use in thin aluminium sheets welding. *Materials & Design*, *30*(5), 1850-1852.
[39] Tian, Y., Shen, J., Hu, S., Liang, Y., & Bai, P. (2018). Effects of ultrasonic peening treatment on surface quality of CMT-welds of Al alloys. *Journal of Materials Processing Technology*, *254*, 193-200.
[40] Su, J., Hu, M., Li, Z., Tang, J., Wang, X., & Luo, Z. (2025). Enhancing mechanical properties and microstructure evaluation in lap welding joint of 5754/6061 dissimilar aluminum alloys via laser-CMT hybrid welding. *Materials Characterization*, 115188.
[41] Feng, J., Zhang, H., & He, P. (2009). The CMT short-circuiting metal transfer process and its use in thin aluminium sheets welding. *Materials & Design*, *30*(5), 1850-1852.
[42] Koli, Y., Yuvaraj, N., & Aravindan, S. (2021). Multi-response mathematical model for optimization of process parameters in CMT welding of dissimilar thickness AA6061-T6 and AA6082-T6 alloys using RSM-GRA coupled with PCA. *Advances in Industrial and Manufacturing Engineering*, *2*, 100050.
[43] Raj, D., Singari, R. M., & Vipin, M. (2022). Study and analyses of arc length correction and mechanical properties on weld bead geometry for AA6061T6 by CMT process. *Materials Today: Proceedings*, *56*, 3475-3483.
[44] Sen, M., Sener, B., & Altan, M. (2020). Effects of process parameters on the formability of sheet metal during plastic injection forming. *Materials Testing*, *62*(5), 535-543.
[45] Yıldırım, E., Çebi, H., Şen, M., & Yılmaz, E. S. (2017). Investigation with Taguchi method of the effects of the robot-controlled induction hardening parameters on surface hardness of sheet metal moulds.
[46] Şen, M., & Altan, M. E. (2017). Plastik enjeksiyon kalıplama yöntemi ile sac metallerin şekillendirilebilirliğinin incelenmesi. *Marmara Fen Bilimleri Dergisi*, *29*(1), 39-47.
[47] Şen, M., & Altan, M. (2017). Sac Metallerin Şekillendirilmesinde Farklı bir Uygulama: Plastik Enjeksiyon Kalıplamada Akışkan Basıncıyla Alüminyum Sacın Şekillendirilmesi. *Çukurova Üniversitesi Mühendislik-Mimarlık Fakültesi Dergisi*, *32*(4), 241-252.
[48] Sen, M., Eryilmaz, O., & Bakir, B. (2024). Multi-objective Process Optimization of Micro-drilling Parameters on Carbon and Carbon–Aramid (Hybrid) Fabric Composites. Arabian Journal for Science and Engineering, 1-18.